Site-Selective Mott Transition in a Quasi-One-Dimensional Vanadate V_6O_{13}

Yasuhiro Shimizu,[1] Satoshi Aoyama,[1] Takaaki Jinno,[1] Masayuki Itoh,[1] and Yutaka Ueda[2,*]
[1]*Department of Physics, Graduate School of Science, Nagoya University, Furo-cho, Chikusa-ku, Nagoya 464-8602, Japan*
[2]*Institute for Solid State Physics, University of Tokyo, Kashiwa, Chiba 277-8581, Japan*

(Received 12 November 2014; published 22 April 2015)

The microscopic mechanism of the metal-insulator transition is studied by orbital-resolved ^{51}V NMR spectroscopy in a prototype of the quasi-one-dimensional system V_6O_{13}. We uncover that the transition involves a site-selective d orbital order lifting twofold orbital degeneracy in one of the two VO_6 chains. The other chain leaves paramagnetic moments on the singly occupied d_{xy} orbital across the transition. The two chains respectively stabilize an orbital-assisted spin-Peierls state and an antiferromagnetic long-range order in the ground state. The site-selective Mott transition may be a source of the anomalous metal and the Mott-Peierls duality.

DOI: 10.1103/PhysRevLett.114.166403 PACS numbers: 71.30.+h, 75.40.Gb, 75.50.-y, 76.60.-k

The metal-insulator transition (MIT) involves several instabilities in quasi-one-dimensional (quasi-1D) systems [1]. A well-known example is a tetragonal (rutile R) phase VO_2 in which a competition of Mott and Peierls instabilities has been actively debated for decades [2–9]. A low-temperature nonmagnetic insulating (monoclinic M_1) phase has a strong dimerization with d orbital ordering along the chain, supporting the orbital-assisted Peierls mechanism of the MIT [10]. The complex phase diagram including a partially paramagnetic insulating (monoclinic M_2) phase under the slight V oxidation [11] or uniaxial stress [12] shows degenerated metastable states arising from the competition of electron correlation and electron-lattice coupling. The underlying physics remains a fundamental issue for strongly correlated systems and practical applications to the Mott transistor [13].

A Wadsley phase V_6O_{13} is another quasi-1D system [14–18] in which the microscopic mechanism of the MIT has been debated for half a century. It has been also extensively studied as a potential cathode in a Li-ion battery [19–21]. There are two frustrated zigzag chains including three vanadium sites, V(1)-V(1) and V(2)-V(3) chains along the b axis, as shown in Fig. 1. A first-order MIT occurs at $T_{\mathrm{MI}} = 150$ K, accompanied by a drop of the magnetic susceptibility χ (Fig. 1) and a weak structural dimerization along the chain [17,22]. The lattice symmetry is lowered from a high-temperature monoclinic $C2/m$ phase to a low-temperature monoclinic Pc phase, doubling vanadium sites [22]. Whereas the nominal valence is $V^{4.33+}(3d^{0.66})$, the V-O bond valence sum suggests nonuniform valence states $V(1)^{+4.26}$, $V(2)^{+4.92}$, and $V(3)^{+4.61}$ even in the metallic phase [17,18]. Similar to the M_2 phase of VO_2 [11], χ remains paramagnetic in the insulating phase, implying a spin-singlet formation for only a part of the vanadium sites [23,24]. Residual local moments exhibit antiferromagnetic long-range ordering at $T_N = 50$ K [24,25].

It is noted that the metallic phase of V_6O_{13} exhibits several anomalous features. χ strongly depends on temperature T above T_{MI} (Fig. 1), implying the presence of local moments. The photoemission spectroscopy shows the depressed density of states at the Fermi level [26–29], suggesting that the spectral weights are partially shifted into lower Hubbard bands due to the strongly renormalized electron correlation. These features are in sharp contrast to those of VO_2 showing the Pauli paramagnetic susceptibility and the appreciable density of states at the Fermi level [11], although T_{MI} in V_6O_{13} is suppressed to the lower

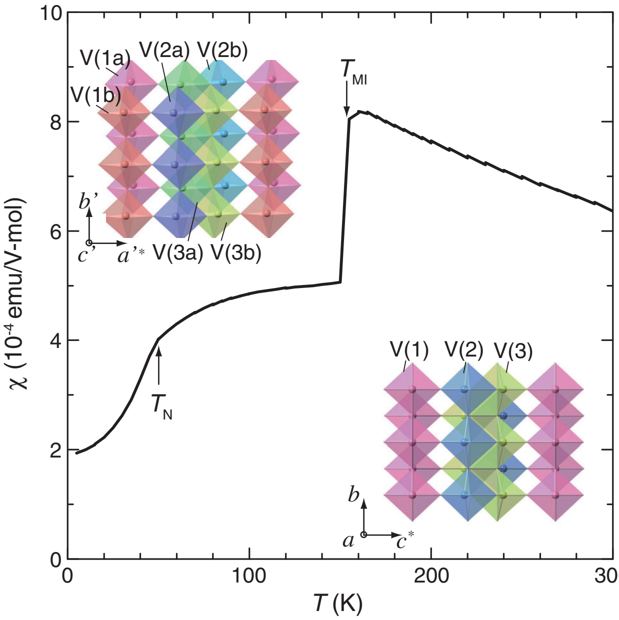

FIG. 1 (color online). Magnetic susceptibility χ measured with a SQUID magnetometer for a single crystal of V_6O_{13} ($H_0 = 1$ T$\|b$ and b'). The lower and upper insets show crystal structures in the metallic (monoclinic $C2/m$) and insulating (monoclinic Pc) phases, respectively [22].

temperature compared to $T_{\mathrm{MI}} = 342$ K in VO_2, possibly due to competing ground states.

In this Letter, we address the microscopic mechanism of MIT and the origin of the anomalous metal in the quasi-1D vanadate. We focus on the orbital degrees of freedom as a key to understanding the MIT for the d electron system, since the electron correlation can be renormalized into d orbital occupations [30]. However, the experimental probe of orbitals has been limited in simple transition-metal compounds [10], and the direct observation of the d orbital for several atomic sites remains challenging. Here, we explore NMR spectroscopy as a site-selective orbital probe by utilizing anisotropic hyperfine interactions. We show a dramatic d orbital ordering across T_{MI} for one of the vanadium sites, while remaining as paramagnetic d_{xy} character for the other sites.

^{51}V NMR measurements were conducted on a single crystal of $\mathrm{V}_6\mathrm{O}_{13}$ made by chemical transport using TeCl_4 [16] and coated with epoxy to prevent crushing at the structural transition. Frequency-swept NMR spectra were obtained from spin-echo signals using a $\pi/2 - \tau - \pi/2$ pulse sequence ($\pi/2 = 1$ μs, $\tau = 5$–30 μs) with a 0.3 MHz step at a constant magnetic field $H_0 = 9.401$ T. For a given orientation of the crystal in H_0, each vanadium site V(i) ($i = 1, 2, 3$ in the metallic phase and $i =$ 1a, 1b, 2a, 2b, 3a, 3b in the insulating phase) gives a set of the ^{51}V NMR spectra at resonance frequencies $\nu_n^{\mathrm{V}(i)} = [1 + K^{\mathrm{V}(i)}]\nu_0 + n\delta\nu^{\mathrm{V}(i)}$ ($n = -3, -2, \ldots, 2, 3$), where $K^{\mathrm{V}(i)}$ are defined as relative shifts from $\nu_0 = 105.23$ MHz and $\delta\nu^{\mathrm{V}(i)}$ is the nuclear quadrupole splitting frequency for the nuclear spin $I = 7/2$. The maximum $|\delta\nu|$ gives the nuclear quadrupole frequency $\nu_Q = 3e^2qQ/h2I(2I-1)$ with Planck's constant h, the nuclear quadrupole moment eQ, and the electric field gradient (EFG) $eq = V_{ZZ}$. The nuclear spin-lattice relaxation rate T_1^{-1} was obtained from a single exponential fit to the recovery curve after an inversion π pulse at a magic angle ($\delta\nu = 0$) for each V site.

Figure 2(a) shows the ^{51}V NMR spectra for $H_0 \| c^*$ (a'^*). In the metallic phase above 150 K, three sets of the spectrum with the characteristic K and $\delta\nu$ are reasonably assigned to three vanadium sites in reference to the expected valences and the symmetry axes of VO_6 distortions. Spike lines located around ν_0 (blue) come from V(2) close to $\mathrm{V}^{5+}(3d^0)$ [24]. The others with the negative K and small (red) or large (green) $\delta\nu$ [Figs. 2(a), 2(b)] are respectively from V^{4+}-like V(1) or V(3) with a weak or strong VO_6 distortion. Below T_{MI}, the number of spectra increases due to the site doubling. A difference in the V(3a) and V(3b) spectra indicates a slight charge transfer between the vanadium sites across T_{MI}. The most noticeable change occurs for the V(1) spectrum: Two sets of the sharp quadrupole split (colored with gray and red) appear with the sizable $\delta\nu$ and vanishing K, indicating the d orbital order, as shown below.

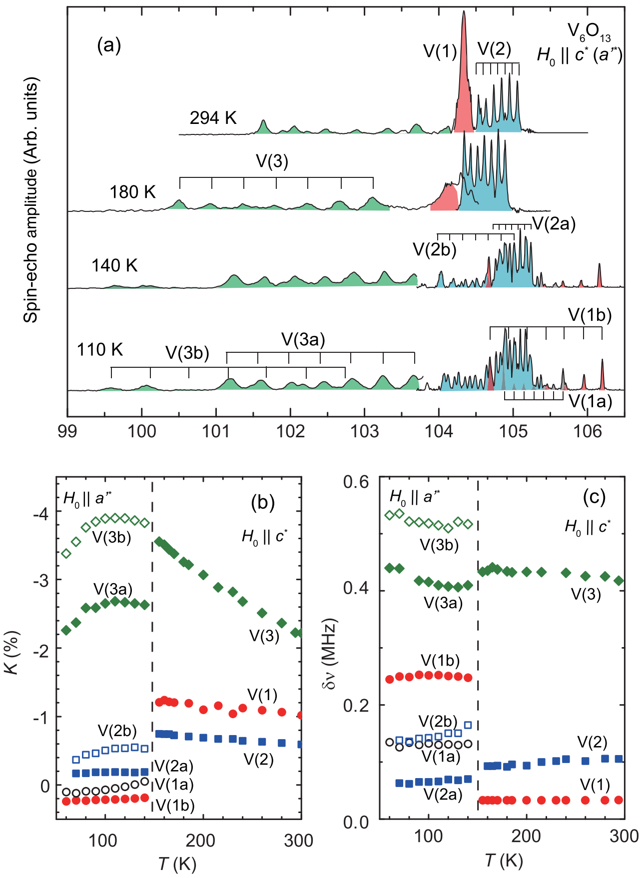

FIG. 2 (color online). (a) ^{51}V NMR spectra of $\mathrm{V}_6\mathrm{O}_{13}$ [$H_0 = 9.401$ T$\|c^*(a'^*)$ for the metallic (insulating) phase], measured with $\tau = 6$ and 10–30 μs for the lower and higher frequency parts, respectively. The red, blue, green, and gray lines are assigned to V(1) [V(1a)], V(2) [V(2a), V(2b)], V(3) [V(3a), V(3b)], and V(1b) based on the angle dependent profiles (Fig. 4). (b) K and (c) $\delta\nu$ obtained from the ^{51}V NMR spectra.

First we focus on the local susceptibility $\chi^{\mathrm{V}(i)}$ for each vanadium site based on K measurements (Fig. S1, Supplemental Material [31]). $\chi^{\mathrm{V}(i)}$ obtained from K is shown in Fig. 3. $\chi^{\mathrm{V}(3)}$ exhibits a strong thermal variation in the metallic phase. It shows a discontinuous increase (decrease) for V(3a) [V(3b)] at T_{MI}. The T dependence behaves similar to that of the spin $S = 1/2$ 1D Heisenberg antiferromagnet ($\mathcal{H} = \sum J\mathbf{S}_i \cdot \mathbf{S}_j$) with an exchange coupling $J = 77$ K for $\chi^{\mathrm{V}(3a)}$ and $\chi^{\mathrm{V}(3b)}$ below 140 K and with $J = 69$ K for $\chi^{\mathrm{V}(3)}$ above 150 K. In contrast, $\chi^{\mathrm{V}(1)}$ exhibits rather weak T dependence in the metallic phase and becomes suppressed in the insulating phase, leaving the small Van Vleck susceptibility [$<5 \times 10^{-4}$ emu/V(1) mol]. The result gives clear evidence for site-selective spin-singlet formations. Namely, the V(1) chain exhibits the MIT from a (Pauli) paramagnetic metal to a nonmagnetic insulator, as seen in VO_2 [11]. $\chi^{\mathrm{V}(2a/2b)}$ becomes negligible below T_{MI}: The on-site d spin is absent on V(2a/2b), rendering V(1a/1b) and V(3a/3b) effectively half-filling.

The dynamical property measured with T_1^{-1} is another manifestation of the site-dependent correlation [Fig. 3(b)].

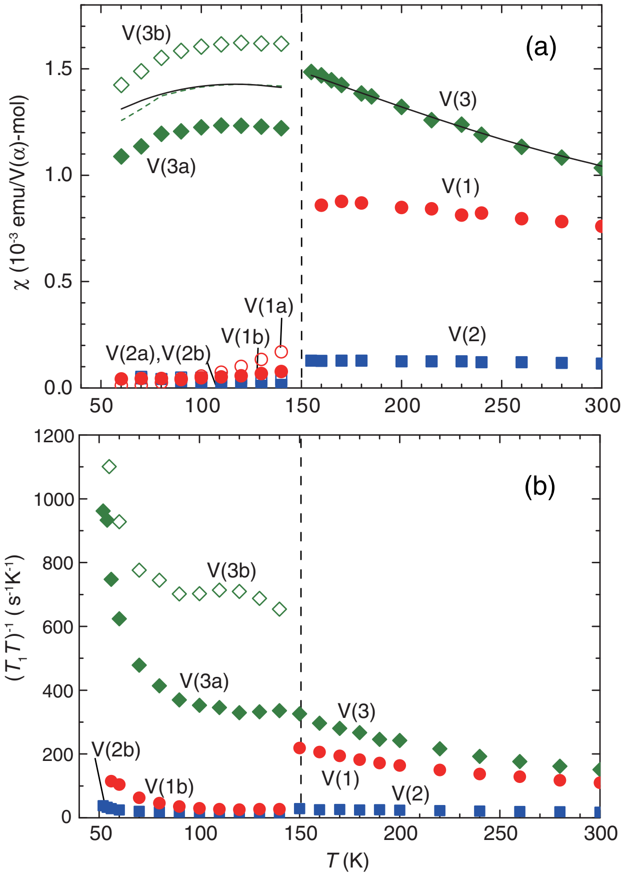

FIG. 3 (color online). (a) Site-dependent local susceptibility obtained from the isotropic ^{51}V Knight shifts and (b) $1/T_1T$ in V_6O_{13}. Solid curves are fitting results of the 1D Heisenberg model, whereas the dashed one is an average of $\chi^{V(3a)}$ and $\chi^{V(3b)}$.

In contrast to weakly correlated metals with the T-linear $1/T_1$, $1/T_1T$ for V(3) increases upon cooling and then becomes further enhanced below $T_{\rm MI}$ for V(3a) and V(3b) due to the evolution of antiferromagnetic fluctuations toward $T_{\rm N}$. For V(1), $1/T_1T$ exhibits a large drop at $T_{\rm MI}$, consistent with the behavior of $\chi^{V(1)}$. Reflecting the dilute spin density, $1/T_1T$ for V(2) is an order of magnitude smaller than those of the other sites. Thus, the site dependence in the spin correlation becomes highlighted below $T_{\rm MI}$.

To give deeper insights into the microscopic origin of the MIT, the predominant d orbital occupation is investigated by measuring the angular dependence of K and $\delta\nu$ (Fig. 4). Since the magnetic susceptibility is isotropic in vanadates, the K and $\delta\nu$ anisotropies are governed by the anisotropic hyperfine couplings expressed with the equivalent operators $\mathsf{q}_{ij} \equiv \frac{3}{2}(L_iL_j + L_jL_i) - \delta_{ij}\mathbf{L}^2$ $(i, j = x, y, z)$ [32,33], where $\mathbf{L}$ represents the total orbital angular momentum in the local coordinates (x, y, z) corresponding to (a, b, c^*) or (c', b', a'^*) (Supplemental Material [31]). One can elucidate orbital occupations by extracting q_{ij}. For a singly occupied d_{xy}, d_{yz}, or d_{zx} orbital, the components of q_{ij} exhibit the cyclic angular dependence [Fig. 4(a)] with a minimum along the symmetry axis of the orbital. For metals, q_{ij} represents the electron cloud distribution for the Hund-coupled bands crossing the Fermi level. With increasing electron correlation, the spin-polarized lower Hubbard band may significantly contribute to the spin susceptibility [30]. On the other hand, q_{ij} obtained from $\delta\nu$ measures the net d occupation below the Fermi level.

As for the metallic phase, $K^{V(3)}$ has a minimum for the c^* axis [Fig. 4(b)], in good agreement with the d_{xy} anisotropy, whereas $K^{V(1)}$ exhibits out-of-phase angular dependence with a maximum for the c^* axis and the depressed anisotropy. q_{ij} is extracted from the spin parts of the axial anisotropy $K^s_{\rm ax}/K^s_{\rm iso}$ and the in-plane asymmetry $K^s_{\rm an}/K^s_{\rm iso}$ expressed with a linear combination of three t_{2g} orbital components $d_{xy}:d_{yz}:d_{zx} = \alpha:\beta:\gamma$ $(\alpha + \beta + \gamma = 1)$, where $K^s_{\rm ax} = (2K^s_Z - K^s_X - K^s_Y)/3$, $K^s_{\rm an} = (K^s_X - K^s_Y)/2$, and $K^s_{\rm iso} = (K^s_X + K^s_Y + K^s_Z)/3$ (Supplemental Material [31]). The obtained occupation ratio is listed in Table I. It turns out that V(1) has an admixture of the d_{yz} and d_{zx} components. It is consistent with the depressed value of $\nu_Q = 0.1$ MHz due to the degenerated orbital occupation (Table S3, Supplemental Material [31]). The results are also in qualitative agreement with a density functional theory (DFT) calculation $(\alpha:\beta:\gamma = 0.0/0.23/0.38)$ [35]. In clear contrast, the V(3) site is mostly polarized to d_{xy}, suggesting strong electron correlations under the crystal field.

On the insulating phase, the angular profiles of K and $\delta\nu$ for V(2a/2b) and V(3a/3b) are similar to those of the metallic phase. It confirms that the orbital states of these sites have less impact on the MIT. The most remarkable change across $T_{\rm MI}$ is the emergence of the huge ν_Q sites, 0.49 MHz for V(1a) and 0.68 MHz for V(1b) [36], pointing to d orbital ordering on the V(1a)-V(1b) chain. The minimum of $\delta\nu$ appears along the b' (c') axis for V(1a) [V(1b)], in agreement with the predominant d_{zx} (d_{yz}) occupation [Figs. 4(a), 4(e)]. Namely, the d_{yz}/d_{zx} degeneracy in the metallic phase is completely lifted by the orbital order. The $\delta\nu$ anisotropy gives the largely polarized occupation for V(1a) and V(1b) (Table I and Supplemental Material Table S3 [31]) after subtracting the lattice contribution (Table S2, Supplemental Material [31]). We thus conclude that the MIT in the present system is attributed to site-selective orbital ordering accompanied by the spin-singlet formation.

The obtained predominant orbitals are depicted in Fig. 5. Owing to the dilute spin density on V(2), the d_{xy} orbitals on the V(3) sites are weakly coupled each other on the V(2)-V(3) zigzag chain and carry the local moments even in the metallic phase. The degenerated d_{yz}/d_{zx} orbitals on V(1) form the conducting chain, which are lifted into the singly occupied d_{yz} or d_{zx} state below $T_{\rm MI}$. A weak dimerization along the V(1a)-V(1b) chain produces the spin-singlet pairs. The π bonding between orthogonal d orbitals should be rather weak. This feature is in clear

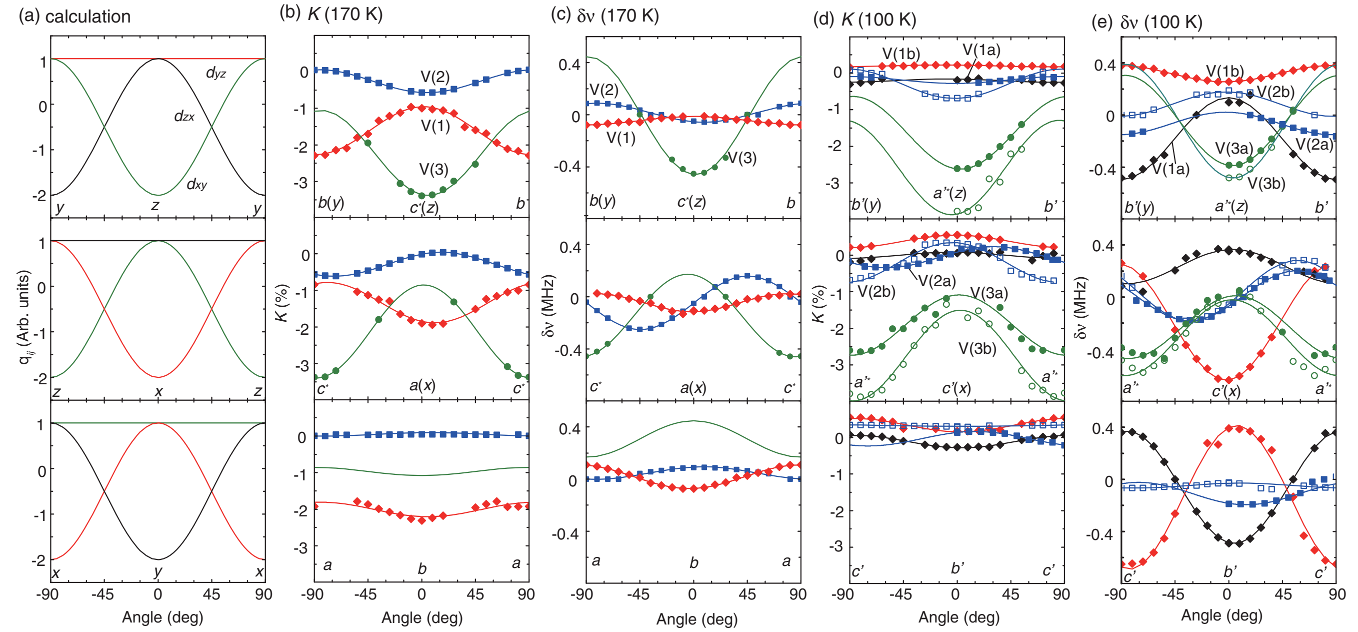

FIG. 4 (color online). (a) Calculated q_{ij} proportional to the on-site dipole hyperfine coupling and EFG for d_{xy}, d_{yz}, and d_{zx} orbitals. The orthogonal coordinate axes (x, y, z) are taken on the VO$_6$ octahedron and parallel to (a, b, c^*) or (c', b', a'^*) in Fig. 1. [(b)–(e)] Angular dependence of the ^{51}V Knight shift K and the nuclear quadrupole splitting frequency $\delta\nu$ at 170 and 100 K in V$_6$O$_{13}$. The curves are fitted results with the sinusoidal functions of Volkov's formula [34].

contrast to the d orbital order in VO$_2$ where the direct d-d σ-bond stabilizes strong spin-singlet pairing [10]. To explain the vanishing spin susceptibility with a sizable spin gap ($\Delta > 150$ K) in V$_6$O$_{13}$, one may have to consider significant superexchange interactions through the O p_z orbital. Such interactions help to lift the d_{yz}/d_{zx} degeneracy, analogous to the Jahn-Teller mechanism [35]. In context, the MIT involves the spin-Peierls transition assisted by orbital ordering and electron-phonon coupling. The above observation of the paramagnetic local moment on V(3a/3b) provides evidence for the Mott insulating ground state of V$_6$O$_{13}$ with antiferromagnetic ordering [24], whereas a theory beyond the DFT + U band calculation [35] is required to describe paramagnetic Mott insulators. It is remarkable that the orbital occupation and the exchange interaction do not show significant changes for V(3) across T_{MI}, keeping the Mott insulating features. The results showing the partially localized vanadium sites are consistent with the depressed spectral weight at the Fermi level and the significant weights well below the Fermi level as observed in the XPS measurements [27].

The site-selective Mott transition has been proposed in rare-earth nickelates based on a DFT + dynamical mean field theory calculation [37], while it has not been confirmed experimentally. Our observations of the site-dependent d occupations and spin susceptibilities give microscopic evidence for the site-selective Mott localization. Many

TABLE I. Axial anisotropy $K^s_{\mathrm{ax}}/K^s_{\mathrm{iso}}$ and in-plane asymmetry $K^s_{\mathrm{an}}/K^s_{\mathrm{iso}}$, the nuclear quadrupole frequency ν_Q, the EFG asymmetry η, and the orbital occupation in V$_6$O$_{13}$, where the occupations are obtained from the K anisotropy for V(i) (i = 1, 3, 1a, 1b, 3a, and 3b) and from the nuclear quadrupole frequency for V(1a) and V(1b) (Supplemental Material [31]).

site	$K^s_{\mathrm{ax}}/K^s_{\mathrm{iso}}$	$K^s_{\mathrm{an}}/K^s_{\mathrm{iso}}$	ν_{Q} (MHz)	η	$d_{xy}:d_{yz}:d_{zx}$
V(1)	−0.38	0.21	0.11	0.40	0.10/0.56/0.28
V(3)	0.77	0.03	0.46	0.26	0.77/0.13/0.10
V(1a)	⋯	⋯	0.49	0.47	0.11/0.18/0.71
V(1b)	⋯	⋯	0.64	0.20	0.13/0.78/0.09
V(3a)	0.70	−0.05	0.44	0.69	0.74/0.16/0.10
V(3b)	0.74	−0.04	0.54	0.76	0.76/0.14/0.10

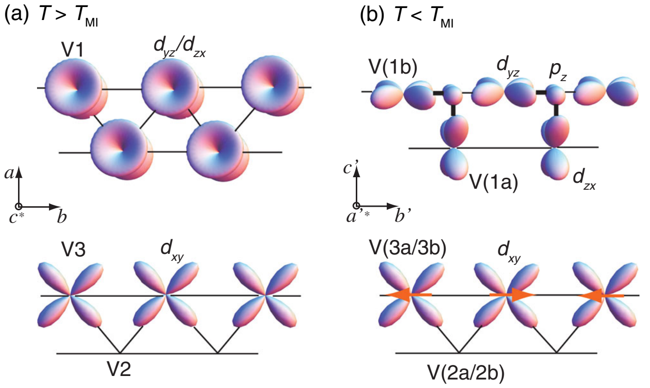

FIG. 5 (color online). Configurations of the predominant orbital occupations in the (a) metallic and (b) insulating phases of V$_6$O$_{13}$. The bold lines indicate spin-singlet pairs. The arrows on V(3a)/V(3b) denote antiferromagnetically ordered spins below 50 K [24].

transition-metal compounds with inequivalent atomic sites have site-dependent local environments and a potential to the site-selective localization, giving anomalous bad metals with the enhanced resistivity and magnetic susceptibility. Even under the weak crystal field, the emergence of the large orbital polarization in the metallic phase may feature the evolution of the lower Hubbard bands. The orbital-resolved NMR provides the site-selective local probe of the orbital order due to strong mass renormalization and can be applied to extensive materials [38].

To conclude, we have presented the observation of the site-selective metal-insulator transition, which accounts for the anomalous features in the historical quasi-one-dimensional correlated system V_6O_{13}. The orbital polarization and local spin susceptibility are elucidated for three vanadium sites with different electron correlations. We uncover that the metal-insulator transition is dominated by orbital ordering and spin-singlet pairing for the itinerant vanadium site with the orbital degeneracy, whereas the magnetic site with the singly occupied orbital remains with paramagnetic moments. Thus the spin-Peierls state and antiferromagnetic order coexist in the insulating ground state. The results demonstrate the competing instabilities and reasonable ways of symmetry breaking in the frustrated one-dimensional system.

We thank Y. Ohta for fruitful discussion and S. Inoue for technical assistance. This work was financially supported by KAKENHI (No. 25610093, No. 23225005, No. 24340080, and No. 25610092) from the Japan Society for the Promotion of Science.

---

[*] Present address: Toyota Physical and Chemical Research Institute, Nagakute 480-1192, Japan.

[1] N. F. Mott, *Metal Insulator Transitions*, 2nd ed. (Taylor and Francis, London, 1990).
[2] F. J. Morin, Phys. Rev. Lett. **3**, 34 (1959).
[3] V. Eyert, Ann. Phys. (Leipzig) **11**, 650 (2002).
[4] J. Goodenough, J. Solid State Chem. **3**, 490 (1971).
[5] A. Zylbersztejn and N. F. Mott, Phys. Rev. B **11**, 4383 (1975).
[6] T. M. Rice, H. Launois, and J. P. Pouget, Phys. Rev. Lett. **73**, 3042 (1994).
[7] S. Biermann, A. Poteryaev, A. I. Lichtenstein, and A. Georges, Phys. Rev. Lett. **94**, 026404 (2005).
[8] M. C. O. Aguiar, V. Dobrosavljevic, E. Abrahams, and G. Kotliar, Phys. Rev. Lett. **102**, 156402 (2009).
[9] C. Weber, D. D. O'Regan, N. D. M. Hine, M. C. Payne, G. Kotliar, and P. B. Littlewood, Phys. Rev. Lett. **108**, 256402 (2012).
[10] M. W. Haverkort, Z. Hu, A. Tanaka, W. Reichelt, S. V. Streltsov, M. A. Korotin, V. I. Anisimov, H. H. Hsieh, H.-J. Lin, C. T. Chen, D. I. Khomskii, and L. H. Tjeng, Phys. Rev. Lett. **95**, 196404 (2005).
[11] J. P. Pouget, H. Launois, T. M. Rice, P. Dernier, A. Gossard, G. Villeneuve, and P. Hagenmuller, Phys. Rev. B **10**, 1801 (1974).
[12] J. P. Pouget, H. Launois, J. P. D'Haenens, P. Merenda, and T. M. Rice, Phys. Rev. Lett. **35**, 873 (1975).
[13] M. Nakano, K. Shibuya, D. Okuyama, T. Hatano, S. Ono, M. Kawasaki1, Y. Iwasa, and Y. Tokura, Nature (London) **487**, 459 (2012).
[14] S. Kachi, K. Takada, and K. Kosuge, J. Phys. Soc. Jpn. **18**, 1839 (1963).
[15] S. Kachi, K. Kosuge, and H. Okinaka, J. Solid State Chem. **6**, 258 (1973).
[16] K. Kawashima, Y. Ueda, K. Kosuge, and S. Kachi, J. Cryst. Growth **26**, 321 (1974).
[17] P. D. Dernier, Mater. Res. Bull. **9**, 955 (1974).
[18] A. C. Gossard, F. J. Di Salvo, L. C. Erich, J. P. Remeika, H. Yasuoka, K. Kosuge, and S. Kachi, Phys. Rev. B **10**, 4178 (1974).
[19] K. West, B. Zachau-Christriansen, T. Jacobsen, and S. Atlung, J. Power Sources **14**, 235 (1985).
[20] M. Y. Saidi, R. Koksbang, E. S. Saidi, H. Shi, and J. Barker, J. Power Sources **68**, 726 (1997).
[21] T. Schmitt, A. Augustsson, J. Nordgren, L.-C. Duda, J. Höwing, T. Gustafsson, U. Schwingenschlögl, and V. Eyert, Appl. Phys. Lett. **86**, 064101 (2005).
[22] J. Höwing, T. Gustafsson, and J. O. Thomas, Acta Crystallogr. Sect. B **59**, 747 (2003).
[23] M. Onoda, T. Ohki, and Y. Uchida, J. Phys. Condens. Matter **16**, 7863 (2004).
[24] M. Itoh, H. Yasuoka, Y. Ueda, and K. Kosuge, J. Phys. Soc. Jpn. **53**, 1847 (1984).
[25] Y. Ueda, K. Kosuge, and S. Kachi, Mater. Res. Bull. **11**, 293 (1976).
[26] S. Shin, S. Suga, M. Taniguchi, M. Fujisawa, H. Kanzaki, A. Fujimori, and H. Daimon, Phys. Rev. B **41**, 4993 (1990).
[27] R. Eguchi, T. Yokoya, T. Kiss, Y. Ueda, and S. Shin, Phys. Rev. B **65**, 205124 (2002).
[28] T. Schmitt, L.-C. Duda, M. Matsubara, M. Mattesini, M. Klemm, A. Augustsson, J.-H. Guo, T. Uozumi, S. Horn, R. Ahuja, A. Kotani, and J. Nordgren, Phys. Rev. B **69**, 125103 (2004).
[29] S. Suga, A. Sekiyama, M. Obara, J. Yamaguchi, M. Kimura, H. Fujiwara, A. Irizawa, K. Yoshimura, M. Yabashi, K. Tamasaku, A. Higashiya, and T. Ishikawa, J. Phys. Soc. Jpn. **79**, 044713 (2010).
[30] M. Imada, A. Fujimori, and Y. Tokura, Rev. Mod. Phys. **70**, 1039 (1998).
[31] See the Supplemental Material at http://link.aps.org/supplemental/10.1103/PhysRevLett.114.166403 for deviations of the local spin susceptibility and orbital occupations.
[32] A. Abragam and B. Bleaney, *Electron Paramagnetic Resonance of Transition Ions* (Oxford University Press, London, 1970).
[33] T. Kiyama and M. Itoh, Phys. Rev. Lett. **91**, 167202 (2003).
[34] G. M. Volkoff, Can. J. Phys. **31**, 820 (1953).
[35] T. Toriyama, T. Nakayama, T. Konishi, and Y. Ohta, Phys. Rev. B **90**, 085131 (2014).
[36] For the site assignment, we referred to directions of the displacements of V ions that determine the *d* orbital state.
[37] H. Park, A. J. Millis, and C. A. Marianetti, Phys. Rev. Lett. **109**, 156402 (2012).
[38] Y. Shimizu, H. Takeda, M. Tanaka, M. Itoh, S. Niitaka, and H. Takagi, Nat. Commun. **3**, 981 (2012).